

Replies to the comments from anonymous referee #3:

We sincerely thank the referee for their thorough review of our manuscript and for raising important points regarding the need for more physics-based interpretation of our results. We appreciate your insights and the opportunity to clarify and strengthen the physical reasoning underlying our analysis. The line changes mentioned in this document correspond to those in the difference file. We have copied the comments into this document; the referee's comments are in Times New Roman blue font while our answers are in Calibri black font.

I read through the author's response document and the revised manuscript. I recognize that the authors have sufficiently addressed most of the questions/comments raised by the reviewers. However, it appears that the current manuscript does not reflect one comment raised by Reviewer #1, and I think it is the most critical comment for considering the publication of this manuscript.

Throughout the manuscript, there are lack of descriptions on a physics-based interpretation of the results. The authors described the results illustrated in Figs very well, compared the results to previous studies, and showed correlation coefficients to "try to" relate the results with some physical parameters. However, correlation coefficients do not help articulate the causality of phenomena. The causality can be inferred based on a physics-based interpretation, otherwise, the discussion does not go beyond a speculative level.

I also argue the robustness of the analysis method related to Figs. 7-8. Lidar ratio, depolarization ratio, and Angstrom exponents are determined by multiple physical variables, not a single hematite fraction. In particular, because hematite is absorptive (i.e., high imaginary refractive index), the authors should stratify the data with particle sizes. This is because the particle absorptivity is primarily determined by a combination of the imaginary refractive index (i.e., degree of absorption in a particle medium) and particle sizes (i.e., a volume or amount of absorbing medium). In this context, the results shown in Table 3 would be helpful. I suggest the authors provide a physical-basis explanation of the results, in particular, a positive correlation of the lidar ratio at 355 nm relating to the imaginary refractive index of hematite, a negative correlation of the Angstrom exponent (355/532) relating to particle size and spectral characteristics of the imaginary refractive index.

In conclusion, the topic is within the scope of ACP, the manuscript has the potential to be publishable if the authors can address the critical comments raised by Reviewer #1 regarding the lack of physics-based explanations/interpretations. I therefore recommend major revisions to consider this manuscript for publication.

From the previous review, we introduced a more explicit physics-based framework in the *Introduction* to aid in interpreting the results. We appreciate the reviewer's observation that this framework had not yet been adequately integrated into the interpretation of the results. In the revised version of the manuscript, we have now expanded the *Results and their discussion* section to fully integrate the physical basis laid out before.

The physics-based framework in our study centers in the relationship between the imaginary part of the refractive index (m_i) and the backscattering coefficient, described by:

$$\beta(\lambda, m) = \int_{D_{max}}^{D_{min}} N(D) \cdot \sigma_{\beta}(m, D, \lambda) dD \quad , \quad (1)$$

where, β is the backscattering coefficient, $N(D)$ is the number concentration of particles of diameter D , and σ_{β} is the backscatter cross-section depending on the complex refractive index ($m = m_R + m_i$), particle size, and wavelength λ .

Mie theory, which assumes spherical particles, is commonly used to calculate the backscatter cross-section. Although this approach does not capture the full complexity of irregularly shaped mineral dust, it provides a reasonable first-order approximation for assessing how the backscatter coefficient responds to variations in the complex refractive index.

We fully acknowledge that particle non-sphericity plays a significant role in shaping dust optical properties. Previous studies have shown that lidar-derived optical properties modeled using Mie theory can differ substantially from observations (Chipade & Pandya, 2023). To address these limitations, more advance scattering optical models that incorporate non-sphericity have been developed, such as those by Dubovik et al. (2006), Gasteiger et al. (2011), Koepke et al. (2015), and Saito and Yang (2021) and Saito et al. (2021). While these models offer increased physical accuracy, discrepancies between modeled and observed data still persist, and the refinement of dust optical modeling remains an active area of research, including ongoing efforts within our own remote sensing group at TROPOS.

Despite the limitations, our rationale for drawing on Mie-theory-derived trends in this study is grounded in its ability to reproduce key relationships that are consistent across more sophisticated scattering models. This is particularly relevant for intensive optical properties, which are independent of aerosol concentration. For example, Wandinger et al. (2023) showed that the backscatter coefficients dependency on the imaginary part of the refractive index (m_i) computed using the spheroidal model of Koepke et al. (2015) closely mirrored those derived from Mie theory. Similarly, Chang et al. (EGUsphere 2024) demonstrated that the negative relationship between m_i and the backscatter coefficient persists regardless of the scattering model employed, whether Mie theory (spheres), the spheroidal model of Dubovik et al. (2006), or the irregular hexahedral model of Saito et al. (2021). To further illustrate this consistency, we include Figure 1 (Fig.5 in Chang et al. (EGUsphere, 2024)) in this answer, which shows that while absolute values differ due to particle shape, the curve of the backscatter coefficient response to increases on m_i remains consistent across models. This convergence supports the robustness of Mie-theory-based trends as a foundation for interpreting the relationships observed in our data.

As part of our physics-based interpretative framework, we refer to Figure 2 in De Leeuw & Lamberts (1987), which presents Mie theory calculations showing that the slope of the β -to- m_i relationship varies by wavelength, with a steeper decline at 532nm compared to 355nm. This behavior is further explained through size parameter considerations ($\chi = 2\pi r/\lambda$): at 355nm, the larger size parameter results in a more forward-peaked scattering pattern, meaning less energy is initially scattered backward relative to 532nm. Consequently, the baseline backscattering is higher at 532nm. As absorption increases through a higher m_i , it dampens internal and surface resonances that enhance backscattering, leading to a more pronounced reduction at 532nm. In contrast, backscatter at 355nm, already lower and less enhanced by resonances is less sensitive to the same increase in absorption. Therefore, under dust particle size regimes and refractive index variations consistent with Di Biagio, et al.

(2019), the steeper decline in backscattering at 532nm reflects its stronger sensitivity to absorption-driven resonance suppression. Although this wavelength-dependent behavior is derived from Mie theory, we consider it robust for interpretation, as the general shape of the backscatter response to increasing m_i is consistent across scattering models. This interpretation is further supported by the behavior of the backscatter-related Ångström exponent shown in Figure 2 in this response (Fig.9 in Chang et al. (EGUsphere, 2024)), which reflects this differential sensitivity of backscattering at the two wavelengths to changes in m_i across scattering models.

Within this framework, we interpret the observed optical variability under the assumption that changes in the modeled hematite fraction are the main driver of variations in the imaginary part of the refractive index. This assumption is supported by the findings of Di Biagio et al. (2019), who demonstrated a positive correlation between hematite content and imaginary refractive index in the UV-Vis spectral range. Their results suggest that even small increases in hematite concentration can significantly influence the optical properties of mineral dust, especially those sensitive to absorption and scattering efficiency.

We use this understanding to interpret the observed relationships between modeled hematite fraction and intensive optical properties. In particular, the backscatter-related Ångström exponent, which depends on the backscatter ratio between 532nm and 355nm reflects the differential sensitivity of each wavelength to increasing m_i . As backscatter at 532nm decreases more steeply than at 355nm with increasing m_i , the ratio $\frac{\beta_{532}}{\beta_{355}}$ approaches unity. Given the definition of the backscatter-related Ångström exponent:

$$\text{ÅE}(\beta)_{355/532} = - \frac{\ln(\frac{\beta_{532}}{\beta_{355}})}{\ln(\frac{532}{355})}, \quad (2)$$

this results in an increase $\text{ÅE}(\beta)_{355/532}$ toward zero, as m_i increases for the cases shown in Figure 7 of the manuscript, where all dust plumes analyzed exhibit a negative $\text{ÅE}(\beta)_{355/532}$. The trend in our data is also consistent with Figure 2 in this response (from Chang et al. (EGUsphere)), which shows that the $\text{ÅE}(\beta)_{355/532}$ with increasing m_i behaves in similar manner across the scattering models.

Additionally, we find that the lidar ratios tend to increase with m_i . This relationship is largely driven by the decline in the backscatter coefficient, since the extinction coefficient is comparatively less sensitive to changes in m_i (Fig.1). While this relationship is not always apparent across the entire dataset, likely due to this property's sensitivity to particle size distributions, it becomes more apparent in the size-segregated analysis (Figure 8 of the manuscript), where internal particle size variability is reduced and compositional effects are more isolated.

We have updated the manuscript to make these interpretative links more explicit. The added discussion clarifies how variations in m_i , linked to hematite content, influence the backscatter coefficient, lidar ratio and Ångström exponent. Furthermore, we have added the slope and intercept of the linear fit in the main results figures in order to facilitate the interpretation of them. The changes can be found in the *Introduction* section between **L60-69** and in the *Results and their discussion* section, particularly sections **3.2.1** and **3.2.2** and in **Figures 7** and **8**.

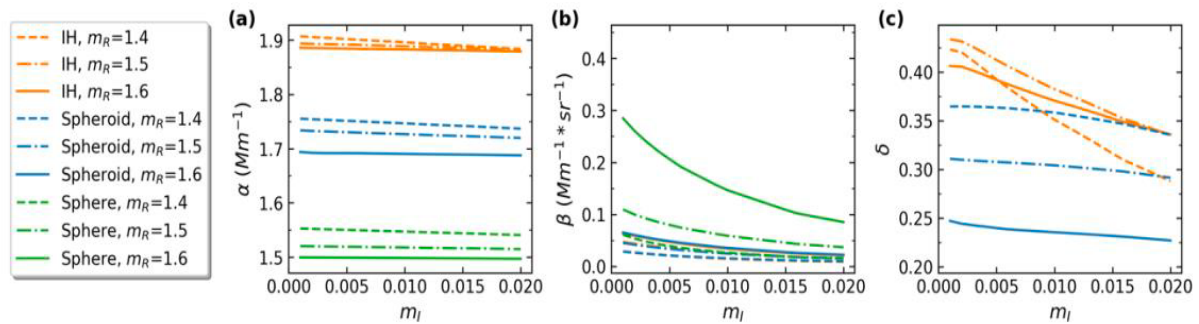


Figure 1. Dependence of (a) extinction coefficient, (b) backscatter coefficient, and (c) particle depolarization ratio on the imaginary part of the refractive index m_i at 532nm, from Chang et al. (EGUsphere2024). Line styles represent different fixed values of the real part of the refractive index ($m_R = 1.4, 1.5$ and 1.6), as indicated in the legend. Colors denote different scattering models: green for spherical particles using Mie theory, blue for spheroids following Dubovik et al. (2006), and orange for irregular hexahedra according to Saito et al. (2021).

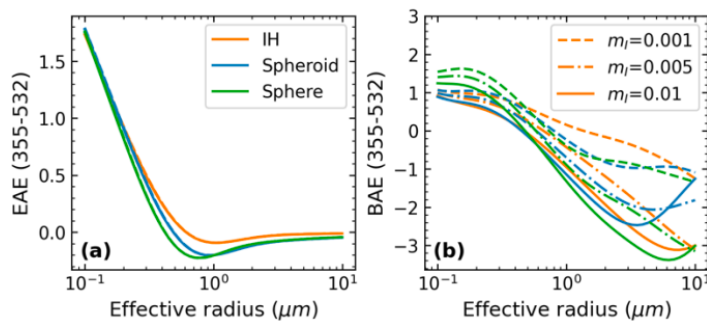


Figure 2. Dependence of the extinction-related Ångström exponent (left) and the backscatter-related Ångström exponent (right) between the 355nm and 532nm wavelengths on the imaginary part of the refractive index m_i from Chang et al. (EGUsphere2024). Line styles represent different fixed values of the imaginary part of the refractive index as indicated in the legend. Colors denote different scattering models as described in Fig.1.

References:

Chang, Y., Hu, Q., Goloub, P., Podvin, T., Veselovskii, I., Ducos, F., Dubois, G., Saito, M., Lopatin, A., Dubovik, O., and Chen, C.: Retrieval of microphysical properties of dust aerosols from extinction, backscattering and depolarization lidar measurements using various particle scattering models, <https://doi.org/10.5194/egusphere-2024-2655>, 2024.

Chipade, R. A. and Pandya, M. R.: Theoretical derivation of aerosol lidar ratio using Mie theory for CALIOP-CALIPSO and OPAC aerosol models, *Atmos. Meas. Tech.*, 16, 5443–5459, <https://doi.org/10.5194/amt-16-5443-2023>, 2023.

De Leeuw, G. and Lamberts, C.: Influence of refractive index and particle size interval on mie calculated backscatter and extinction, *Journal of Aerosol Science*, 18, 131–138, [https://doi.org/10.1016/0021-8502\(87\)90050-4](https://doi.org/10.1016/0021-8502(87)90050-4), 1987.

Di Biagio, C., Formenti, P., Balkanski, Y., Caponi, L., Cazaunau, M., Pangui, E., Journet, E., Nowak, S., Andreae, M. O., Kandler, K., Saeed, T., Piketh, S., Seibert, D., Williams, E., and Doussin, J.-F.: Complex refractive indices and single-scattering albedo of global dust aerosols in the shortwave spectrum and relationship to size and iron content, *Atmos. Chem. Phys.*, 19, 15503–15531, <https://doi.org/10.5194/acp-19-15503-2019>, 2019.

Dubovik, O., Sinyuk, A., Lapyonok, T., Holben, B. N., Mishchenko, M., Yang, P., Eck, T. F., Volten, H., Muñoz, O., Veihelmann, B., Van Der Zande, W. J., Leon, J., Sorokin, M., and Slutsker, I.: Application of spheroid models to

account for aerosol particle nonsphericity in remote sensing of desert dust, *Journal of Geophysical Research: Atmospheres*, 111, 2005JD006 619, <https://doi.org/10.1029/2005JD006619>, 2006.

Gasteiger, J., Wiegner, M., Groß, S., Freudenthaler, V., Toledano, C., Tesche, M., and Kandler, K.: Modelling lidar-relevant optical properties of complex mineral dust aerosols, *Tellus B*, 63, 725–741, <https://doi.org/10.1111/j.16000889.2011.00559.x>, 2011.

Koepke, P., Gasteiger, J., and Hess, M.: Technical Note: Optical properties of desert aerosol with non-spherical mineral particles: data incorporated to OPAC, *Atmos. Chem. Phys.*, 15, 5947–5956, <https://doi.org/10.5194/acp-15-5947-2015>, 2015.

Saito, M. and Yang, P.: Advanced Bulk Optical Models Linking the Backscattering and Microphysical Properties of Mineral Dust Aerosol, *Geophysical Research Letters*, 48, e2021GL095 121, <https://doi.org/10.1029/2021GL095121>, 2021.

Saito, M., Yang, P., Ding, J., and Liu, X.: A comprehensive database of the optical properties of irregular aerosol particles for radiative transfer simulations, *Journal of the Atmospheric Sciences*, <https://doi.org/10.1175/JAS-D-20-0338.1>, 2021.

Wandinger, U., Floutsi, A. A., Baars, H., Haarig, M., Ansmann, A., Hünerbein, A., Docter, N., Donovan, D., Van Zadelhoff, G.-J., Mason, S., and Cole, J.: HETEAC – the Hybrid End-To-End Aerosol Classification model for EarthCARE, *Atmospheric Measurement Techniques*, 16, 2485–2510, <https://doi.org/10.5194/amt-16-2485-2023>, 2023.